ORGANOMETALLICS
Communication
Cite This: Organometallics 2019, 38, 4054−4059
pubs.acs.org/Organometallics

Siloxide Podand Ligand as a Scaffold for Molybdenum-Catalyzed Alkyne Metathesis and Isolation of a Dynamic Metallatetrahedrane Intermediate

Richard R. Thompson,[†] Madeline E. Rotella,[‡] Pu Du,[†] Xin Zhou,[†] Frank R. Fronczek,[†] Revati Kumar,[†] Osvaldo Gutierrez,*[,‡] and Semin Lee*[,†]

[†]Department of Chemistry, Louisiana State University, Baton Rouge, Louisiana 70810, United States
[‡]Department of Chemistry and Biochemistry, University of Maryland, College Park, Maryland 20742, United States

Supporting Information

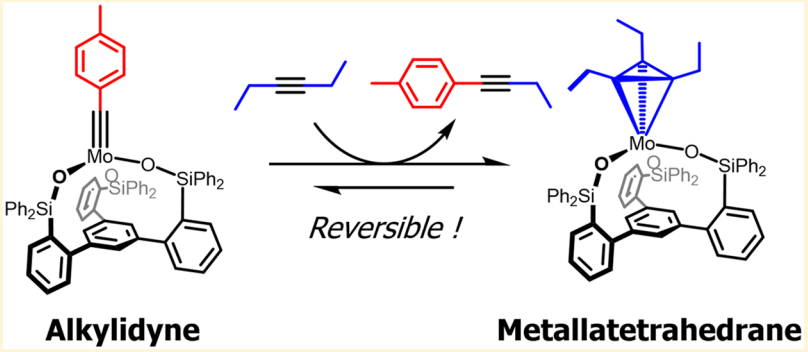

ABSTRACT: Triphenylsiloxide is one of the most successful ancillary ligands for Mo(VI)-alkyne metathesis catalysts. It was proposed that flexible siloxide ligands allow Mo−O−Si bond angles to modulate the electrophilicity of Mo≡C and thereby promote the catalysis. Introduction of a siloxide podand ligand allowed elucidation of the effect of ligand flexibility and Mo−O−Si angles on the electrophilicity of Mo≡C. It also allowed for the isolation of a rare metallatetrahedrane of Mo(VI) which was found to be dynamic in solution.

Alkyne metathesis, the metal-catalyzed exchange of carbon−carbon triple bonds, has encountered a renaissance[1,2] 50 years after its initial discovery.[3,4] The growing interest is due to its applications in fields as diverse and important as natural product synthesis,[5−7] supramolecular chemistry,[8−19] and polymer science.[20−25] Oftentimes the synthetic targets were otherwise inaccessible or could only be produced by multistep methods in low yields.[26−28] Such fields would benefit from catalysts with better substrate tolerance, higher activity, and longer lifetimes. Progress has been made in predicting and understanding means for catalyst improvements, including the "push-pull mechanism" posited by Tamm[29,30] or the blocking of open coordination sites inhibiting 2-butyne polymerization presented by Zhang.[31−33] Much work, however, remains in developing the same level of systematic advancements seen for subfields such as olefin metathesis.[34,35]

One of the most successful ancillary ligands for alkyne metathesis is triphenylsiloxide, established by Fürstner (Figure 1a, [**Mo**]$\mathbf{L_3}$).[36−38] This system is active at low catalyst loading with high turnover frequencies and reasonable functional group tolerance, including the cross-metathesis of certain terminal alkynes.[39] Remarkably, the precatalyst [**Mo**]$\mathbf{L_3}$**phen** is air- and moisture-stable and can be readily activated upon exposure to $MnCl_2$ or $ZnCl_2$. Of considerable importance within [**Mo**]$\mathbf{L_3}$ is the observed acuteness of the Mo−O−Si bond angle, which has been proposed to reduce the extent of π donation from the O lone pairs into the empty Mo d orbitals (Figure 1c, BENT).[1] Fürstner suggested that acute Mo−O−Si angles render the metal center more electrophilic and encourage the formation of the metallacyclobutadiene (MCBD) intermediate. Subsequent straightening of the Mo−O−Si angle then drives product release to regenerate the alkylidyne functionality (Figure 1c, LINEAR). Principal to this design element, therefore, is the flexibility of the Mo−siloxide bond to sample a wide range of angles. A conceptually simple means for probing this importance would be to limit flexibility by tethering the three Ph_3SiO groups together as a single, tridentate chelate.

Fürstner, partially inspired by the work of Zhang,[31−33] previously attempted to utilize tridentate siloxide ligands for chelating Mo(VI)-alkylidynes.[6] However, due to the flexible alkyl linkers, the ligands preferred the formation of poorly defined oligomeric species. Herein, we suggest the use of the structurally preorganized siloxide podand ligand **SiP** (Figure

Received: June 26, 2019
Published: October 28, 2019

DOI: 10.1021/acs.organomet.9b00430
Organometallics 2019, 38, 4054−4059

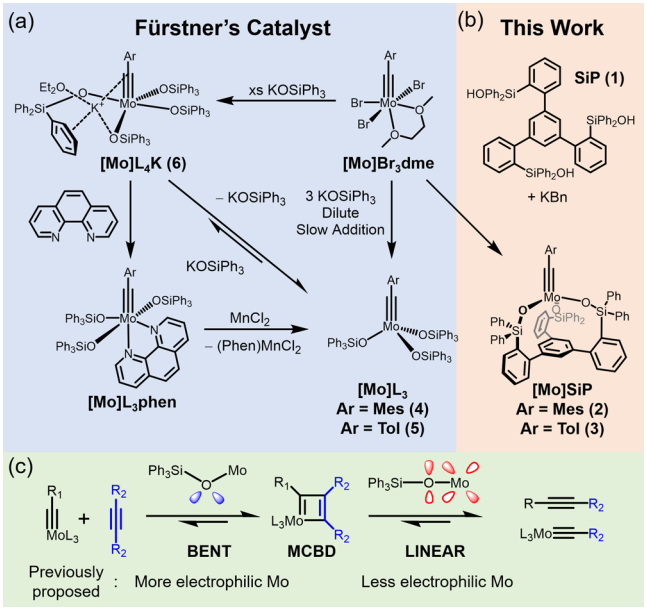

Figure 1. (a) Synthesis of Fürstner's catalyst. (b) Catalyst in this work. (c) Current explanation for the role Mo–O–Si bond angle plays in catalyst activity.

1b) and its successful coordination to molybdenum alkylidynes [**Mo**]**SiP**. We directly compare the spectroscopic, structural, and catalytic properties of these compounds versus those of their nonchelating [**Mo**]$\mathbf{L_3}$ analogues and rationalize their differences in electrophilicity and performance as the result of reduced flexibility.

The podand precursor $C_6H_3(C_6H_4Br)_3$[40] was treated with *t*-BuLi followed by the addition of Ph_2SiCl_2.[41] An aqueous workup resulted in the podand ligand **1** in good yields. The ^{1}H NMR spectrum of **1** revealed a Si–O*H* resonance at 4.45 ppm, indicative of intramolecular hydrogen bond formation among the silanol moieties. An X-ray crystallographic analysis of **1** clearly confirmed that all Si–O bonds were directed toward the center (Figure S22). In situ generation of the trianionic potassium salt of **1** via treatment with 3 equiv of benzylpotassium (KBn) in THF followed by addition of [**Mo**]**Br$_3$dme** (Ar = mesityl, tolyl) allowed for the isolation of the [**Mo**]**SiP** complexes **2** (Ar = mesityl) and **3** (Ar = tolyl) as orange and yellow powders, respectively (Figure 1b). Following procedures similar to those reported by Fürstner (Figure 1a), the analogous triphenylsiloxide catalysts ([**Mo**]$\mathbf{L_3}$) **4** (Ar = mesityl) and **5** (Ar = tolyl) were prepared. As seen for Fürstner, the preparation of **5** required the use of highly dilute conditions to avoid the formation of the pentacoordinate salt [**Mo**]$\mathbf{L_4K}$ (**6**), which was also synthesized and characterized as an etherate. ^{1}H and ^{13}C NMR spectrometry of **2**–**5** revealed them to be C_3 symmetric.

The catalytic activities of **2**–**5** were examined by monitoring the dynamic scrambling of 1-methoxy-4-(phenylethynyl)-benzene (Figure 2) with 2% catalyst loading at room temperature. The reaction progress was monitored by using the ^{1}H NMR chemical shift of methoxy OC*H*$_3$ as a spectroscopic handle. In the case of **2**, no reaction was observed up to 12 h at room temperature; however, heating to 75 °C allowed the reaction to reach equilibrium within 2.5 h. The persistence of mesityl resonances associated with **2** throughout the time of the reaction suggested an incomplete initiation of the catalyst. Conversely, catalyst **3**, with a sterically

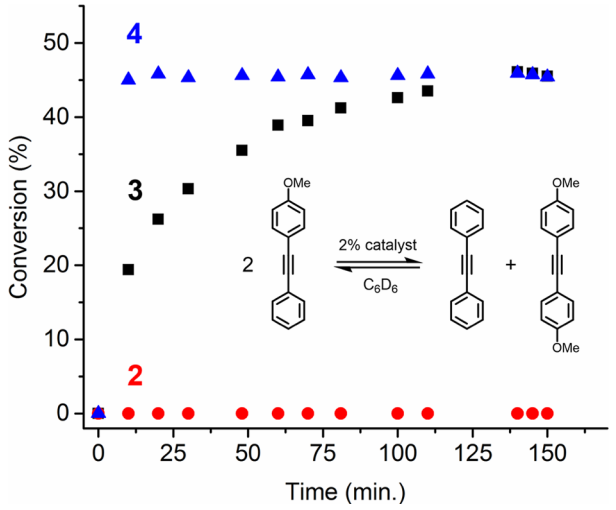

Figure 2. Dynamic scrambling of 1-methoxy-4-(phenylethynyl)-benzene (0.4 mM in C_6D_6) catalyzed by 2 mol % of **2**–**4** at room temperature monitored by ^{1}H NMR.

less encumbered tolyl group, was capable of reaching equilibrium within 2.5 h at room temperature, thus signifying that **SiP**-supported molybdenum alkylidynes can catalyze metathesis at ambient temperature. Reactions catalyzed by **4** and **5** both reached equilibrium within <10 min, regardless of the initial aryl group. To better understand the discrepancies in activity among the catalysts, we first turned to structural and spectroscopic studies.

Single crystals for X-ray crystallography were obtained by slow evaporation of ethereal solutions of catalysts **2**–**5** (Figure 3). Mo≡C1 bond lengths range from 1.741 to 1.749 Å among the four structures. Noticeable differences among **2**–**5** were that Mo–O bond lengths are shorter and Mo–O–Si bond angles are more linear in the [**Mo**]**SiP** systems **2** and **3** in comparison to the [**Mo**]$\mathbf{L_3}$ systems **4** and **5**. Interestingly, the three Mo–O–Si angles in **2** and **3** had less variance (161.6–172.2° and 161.9–166.5°, respectively) in comparison to those in **4** and **5** (141.4–173.5 and 139.9–160.2°, respectively), which indirectly suggests that the podand ligand restricts the flexibility of the $-OSiPh_2$ groups.

Next, we investigated the effect of ligand geometry on the electrophilicity of the Mo≡C group. Recently, Tamm and Coperet used the ^{13}C chemical shift of Mo≡C as a probe for the electrophilicity of Mo and alkyne metathesis activity of structurally related catalysts.[42] As expected, increased electrophilicity improved activity, promoting the rate-limiting [2 + 2] cycloaddition. However, excessively electron withdrawing ligands (i.e., $-OC(CF_3)_3$) made the metal too electrophilic and overstabilized the MCBD enough to a point that retro-[2 + 2] cycloaddition became rate-limiting, substantially reducing catalyst activity.[43] To probe possible electronic differences between [**Mo**]**SiP** and [**Mo**]$\mathbf{L_3}$, we compared the Mo≡C ^{13}C chemical shifts. The current paradigm (Figure 1c) would suggest that more linear Mo–O–Si bond angles in **2** and **3** would result in less electrophilic Mo centers and thus less deshielded carbynes. Surprisingly, **2** and **3** were *more* deshielded relative to **4** and **5** by 4.9 and 10.4 ppm, respectively (Figure 3).

To understand the role that ligand geometry has on electronic properties of the molybdenum-carbyne and ^{13}C carbyne chemical shift, we turned to dispersion-corrected

DOI: 10.1021/acs.organomet.9b00430
Organometallics 2019, 38, 4054–4059

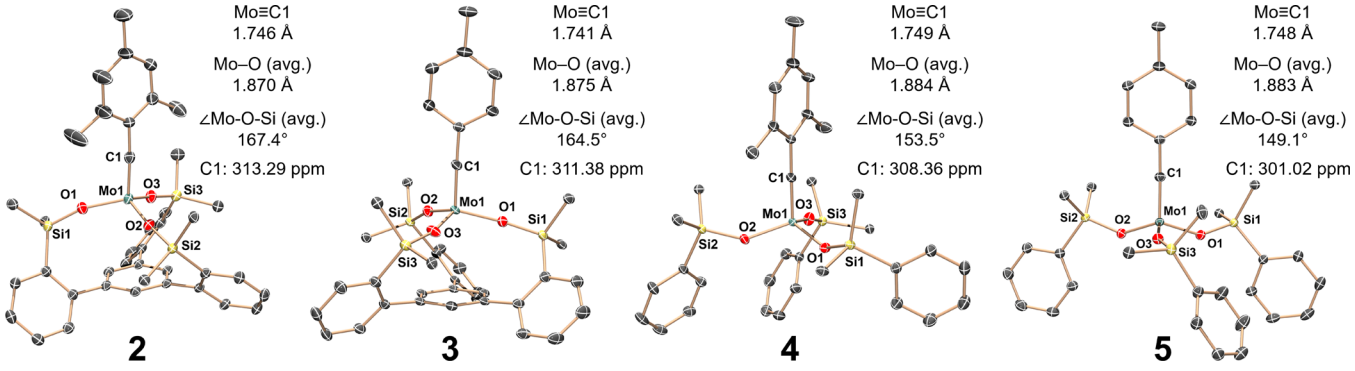

Figure 3. Molecular structures of compounds **2**–**5** showing thermal ellipsoids at the 50% probability level with H atoms, solvent, and peripheral phenyl groups omitted for clarity. ^{13}C NMR resonances of Mo-carbynes (C1) are indicated.

density functional theory calculations (B3LYP-D3/defTZVP-SDD(Mo)-CPCM(benzene)//B3LYP-D3/def2SVP-LANL2DZ(Mo)-CPCM(benzene)) (see the Supporting Information for computational details). For both of the optimized structures $\mathbf{3}_{calc}$ and $\mathbf{5}_{calc}$ the core experimental geometries are in reasonable agreement with computations (Mo−O−Si average 164.5 vs 160.0° for **3** and 149.1 vs 146.2° for **5**), although the Mo−O−Si angles in each were found to be more acute (Figures S29 and S30), suggesting that crystal-packing forces may cause these angles to distort from ideal geometry. Next, we systematically changed one of the Mo−O−Si bond angles of both catalysts to probe its effect on Mulliken charges and ^{13}C carbyne chemical shifts. By monitoring Mulliken charges, we found that as one of the Mo−O−Si angles becomes more linearized from 135 to 175°, the electron densities of the carbyne carbon and oxygen decrease, while that of molybdenum increases (Figures S32 and S33). On the other hand, linearization of one of the Mo−O−Si bond angles did not result in a significant change in the calculated carbyne ^{13}C chemical shifts of **3** and **5** (Figure S31). In a separate calculation, we locked all three siloxide angles of **5** into linearized (178°) geometries ($\mathbf{5}_{178°}$, Figure S34). Such a geometry resulted in an intermediate chemical shift (^{13}C 320.99 ppm) and Mulliken charges (C −0.69, Mo +1.87) which lie between those of $\mathbf{3}_{calc}$ and $\mathbf{5}_{calc}$. Taken together, this result suggests that, while the Mo−O−Si angle contributes to carbyne ^{13}C chemical shifts, it is not the primary factor for explaining the intrinsic difference between **3** and **5**.

Careful inspection of the solid-state structures of **3** and **5** reveals that tethering the three siloxides via the basal arene results in a considerable distortion of the ligand geometry about the metal. Specifically, the average of the C≡Mo−O−Si dihedral angles of **3** (106.1°) was significantly larger than that of **5** (35.6°), a trend which was reproduced in silico: $\mathbf{3}_{calc}$ (105.7°) and $\mathbf{5}_{calc}$ (16.3°). To probe the effect of this conformational difference, the geometry of $\mathbf{5}_{calc}$ was constrained to match that of $\mathbf{3}_{calc}$ (i.e., $\mathbf{5}_{constrained}$; Figure S36). This resulted in nearly identical carbyne ^{13}C chemical shifts and Mo Mulliken charges between those of $\mathbf{3}_{calc}$ (330.02 ppm, +1.86) and $\mathbf{5}_{constrained}$ (328.73 ppm, +1.84). This suggests that the overall geometry imparted by the **SiP** scaffold is the greater determinant of electrophilicity, as assayed by the calculated carbyne ^{13}C chemical shifts. Further computational studies on orbital interactions between the ligands and Mo-carbyne are forthcoming to clearly tease out the impact of each geometric factor.[44]

Previous work by Tamm has shown that increased electrophilicity can result in the isolation of MCBD intermediates.[43,45] In order to test if **3** could allow for similar stabilization, we treated it with 5 equiv of 3-hexyne (Figure 4).[45] ^{1}H NMR studies revealed the production of the expected

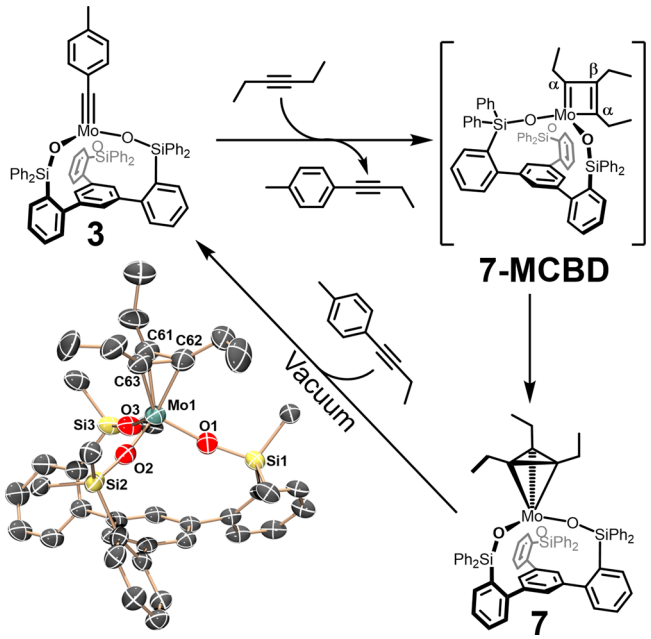

Figure 4. Chemically reversible cycle for the interconversion of alkylidyne **3** with the metallatetrahedrane **7**, by addition and removal of 3-hexyne. The molecular structure of metallatetrahedrane **7** shows thermal ellipsoids at the 50% probability level with H atoms, disordered groups, and peripheral phenyl groups omitted for clarity.

organic product, 1-*p*-tolylbut-1-yne, along with a new organometallic species which retained C_3 symmetry and a single ethyl environment. ^{13}C NMR studies at both room temperature and −70 °C failed to give evidence of either C_α (~250 ppm) or C_β (~140 ppm) resonances of a MCBD. Instead, a chemical shift of 84.45 ppm was located and correlated to the organometallic ethyl species (Figures S14–S17). Taken together, the observed spectra indicates the full conversion of **3** into a rare example of a metallatetrahedrane, **7** (Figure 4).[46−50] The preparation of **7** in pentane followed by storage at −37 °C over the course of 6 weeks led to the production of crystals suitable for X-ray diffraction. Assuming the C_3Et_3 fragment occupies a single coordination site, **7** can be thought of as pseudotetrahedral,

DOI: 10.1021/acs.organomet.9b00430
Organometallics 2019, 38, 4054−4059

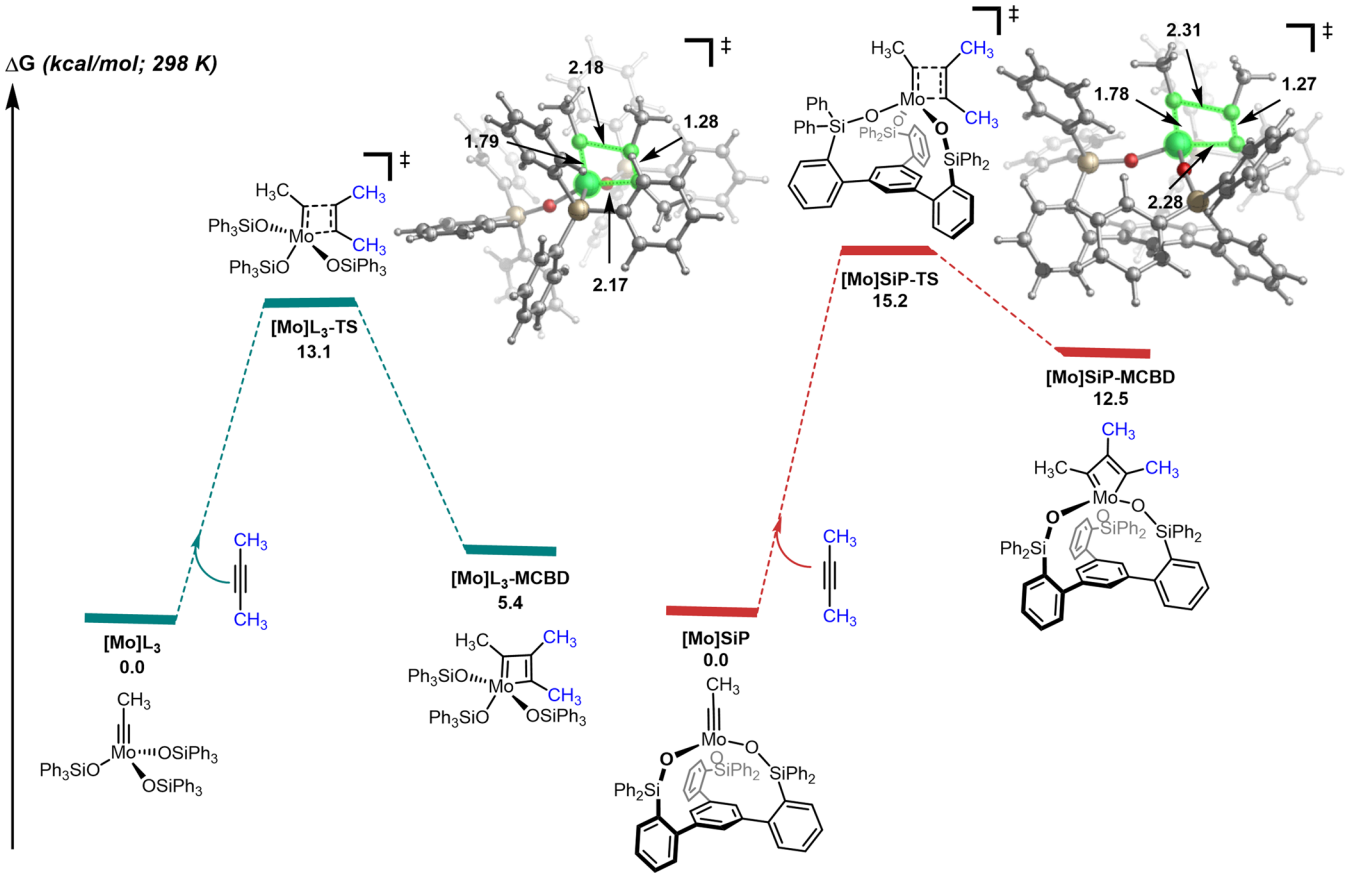

Figure 5. Energetics of MCBD formation via [2 + 2] cycloaddition for [**Mo**]L_3 (left, green) and [**Mo**]**SiP** (right, red). Free energies (kcal/mol) are computed at the B3LYP-D3/defTZVP-SDD(Mo)-CPCM(benzene)//B3LYP/LANL2DZ level of theory. For enthalpy and electronic energies, refer to Figure S36.

which is unique relative to all other group VI analogues, which have been six-coordinate or higher. The Mo−C_3Et_3 centroid distance of **7**, 1.884 Å, is the shortest distance for group VI species[46,47,51] and is dramatically shorter than those for the only other crystallographically characterized Mo species (2.056−2.067 Å),[49,50] which are all donor−acceptor pairs between a low-valent metal and cyclopropyllium fragments and thus are chemically distinct.

Historically, metallatetrahedranes have been viewed as thermodynamic sinks and deactivation pathways for alkyne metathesis catalysts.[52] Surprisingly, treatment of the reaction mixture with vacuum resulted in the full reversion of **7** to **3** (Figure 4a and Figure S18). Even more impressively, 4-tolylpropyne was found to undergo alkyne metathesis in the presence of **7** and residual 3-hexyne (Figures S19 and S20). This shows that not only is the metallatetrahedrane not a permanent decomposition pathway but also it is dynamic enough to participate in alkyne metathesis.

To further compare the activity of the two ligand sets, the reaction coordinates of both [**Mo**]L_3 and [**Mo**]**SiP** with acetylene (Figure S35), as well as 2-butyne (Figure 5), were modeled as simplified systems for a preliminary mechanistic study. Using acetylene as the substrate, calculations predict nearly identical barriers for the [2 + 2] cycloaddition between acetylene and [**Mo**]L_3 and [**Mo**]**SiP**: 12.8 and 12.0 kcal/mol, respectively (Figure S35). Notably, the barrier associated with [**Mo**]L_3 is slightly higher, suggesting that the ligand geometry of **SiP** may be beneficial in the cross-metathesis of sterically unhindered, unsubstituted alkynes. Upon an increase in the steric bulk of the model to ethylidynes reacting with 2-butyne, the [2 + 2] cycloaddition transition state from the [**Mo**]**SiP** system was found to be 2.1 kcal/mol higher in energy than that for the [**Mo**]L_3 system (Figure 5), supporting the experimental results. Furthermore, there is a significant destabilization of the MCBD of [**Mo**]**SiP** relative to [**Mo**]L_3, likely as a result of steric clashing between the methyl groups of the MCBD and the phenyl groups of the ligand (Figure S37). These preliminary results suggest that, as the steric bulk of the substrate increases, the energies of the initial [2 + 2] transition state and corresponding MCBD adduct increase as a consequence of steric interactions between the substrate and the more rigid ligand in [**Mo**]**SiP**. Finally, the metallatetrahedrane (MTd) motif was found more stable than the MCBD analogue by 11.2 kcal/mol and was nearly isoenergetic with the [**Mo**]**SiP** alkylidyne, in a calculated model system (Figure S38). More detailed computational studies are underway to rationally design siloxide podand-Mo complexes for faster alkyne metathesis.

To conclude, by tethering three Ph_3SiO ligands together with a single arene linker, we have given greater insight into the role the siloxide ligand geometry has on catalyst activity and electrophilicity. We further discovered that treatment of the SiP-supported alkylidyne with a slight excess of 3-hexyne resulted not in the expected MCBD intermediate but rather in a rare instance of a molybdenum metallatetrahedrane. Finally, this species was found to be dynamic, by both being able to revert to the original alkylidyne under vacuum and being able to participate in alkyne metathesis.

DOI: 10.1021/acs.organomet.9b00430
Organometallics 2019, 38, 4054−4059

■ ASSOCIATED CONTENT

Supporting Information

The Supporting Information is available free of charge on the ACS Publications website at DOI: 10.1021/acs.organomet.9b00430.

Experimental procedures, NMR spectral data, crystallographic data, and computational details (PDF)

Cartesian coordinates for the calculated structures (XYZ)

Accession Codes

CCDC 1936239−1936244 and 1951303 contain the supplementary crystallographic data for this paper. These data can be obtained free of charge via www.ccdc.cam.ac.uk/data_request/cif, or by emailing data_request@ccdc.cam.ac.uk, or by contacting The Cambridge Crystallographic Data Centre, 12 Union Road, Cambridge CB2 1EZ, UK; fax: +44 1223 336033.

■ AUTHOR INFORMATION

Corresponding Authors

*E-mail for O.G.: ogs@umd.edu.
*E-mail for S.L.: seminlee@lsu.edu.

ORCID

Richard R. Thompson: 0000-0002-2181-9846
Madeline E. Rotella: 0000-0002-7973-2452
Xin Zhou: 0000-0003-1531-8698
Frank R. Fronczek: 0000-0001-5544-2779
Revati Kumar: 0000-0002-3272-8720
Osvaldo Gutierrez: 0000-0001-8151-7519
Semin Lee: 0000-0003-0873-9507

Notes

We note that a closely related catalyst with a ligand identical with **SiP** was reported by Fürstner and co-workers after the submission of this work.[53]

The authors declare no competing financial interest.

■ ACKNOWLEDGMENTS

This research was supported by the College of Science and the Office of Research and Economic Development at Louisiana State University. R.R.T. and S.L. also thank Prof. Felix Fischer and Dr. Stephen von Kugelgen for helpful discussions concerning the synthesis and purification of [**Mo**]Br_3**dme** as well as Dr. Scott Smith for the use of the University of Houston NMR facilities. O.G. is grateful to the University of Maryland College Park for start-up funds and computational resources from UMD Deepthought2 and MARCC/BlueCrab HPC clusters and XSEDE (CHE160082 and CHE160053). Further, O.G. is grateful for financial support by the NSF (CAREER 1751568).

■ REFERENCES

(1) Furstner, A. Alkyne metathesis on the rise. *Angew. Chem., Int. Ed.* **2013**, *52*, 2794−2819.
(2) Ehrhorn, H.; Tamm, M. Well-Defined Alkyne Metathesis Catalysts: Developments and Recent Applications. *Chem. - Eur. J.* **2018**, *25*, 3190−3208.
(3) Pennella, F.; Banks, R. L.; Bailey, G. C. Disproportionation of alkynes. *Chem. Commun.* **1968**, 1548−1549.
(4) Mortreux, A.; Blanchard, M. Metathesis of alkynes by a molybdenum hexacarbonyl−resorcinol catalyst. *J. Chem. Soc., Chem. Commun.* **1974**, 786−787.
(5) Meng, Z.; Fürstner, A. Total Synthesis of (−)-Sinulariadiolide. A Transannular Approach. *J. Am. Chem. Soc.* **2019**, *141*, 805−809.
(6) Schaubach, S.; Gebauer, K.; Ungeheuer, F.; Hoffmeister, L.; Ilg, M. K.; Wirtz, C.; Fürstner, A. A Two-Component Alkyne Metathesis Catalyst System with an Improved Substrate Scope and Functional Group Tolerance: Development and Applications to Natural Product Synthesis. *Chem. - Eur. J.* **2016**, *22*, 8494−8507.
(7) Hötling, S.; Bittner, C.; Tamm, M.; Dähn, S.; Collatz, J.; Steidle, J. L. M.; Schulz, S. Identification of a Grain Beetle Macrolide Pheromone and Its Synthesis by Ring-Closing Metathesis Using a Terminal Alkyne. *Org. Lett.* **2015**, *17*, 5004−5007.
(8) Gross, D. E.; Moore, J. S. Arylene−Ethynylene Macrocycles via Depolymerization−Macrocyclization. *Macromolecules* **2011**, *44*, 3685−3687.
(9) Lee, S.; Chénard, E.; Gray, D. L.; Moore, J. S. Synthesis of Cycloparaphenyleneacetylene via Alkyne Metathesis: C70 Complexation and Copper-Free Triple Click Reaction. *J. Am. Chem. Soc.* **2016**, *138*, 13814−13817.
(10) Lee, S.; Yang, A.; Moneypenny, T. P.; Moore, J. S. Kinetically Trapped Tetrahedral Cages via Alkyne Metathesis. *J. Am. Chem. Soc.* **2016**, *138*, 2182−2185.
(11) Moneypenny, T. P.; Yang, A.; Walter, N. P.; Woods, T. J.; Gray, D. L.; Zhang, Y.; Moore, J. S. Product Distribution from Precursor Bite Angle Variation in Multitopic Alkyne Metathesis: Evidence for a Putative Kinetic Bottleneck. *J. Am. Chem. Soc.* **2018**, *140*, 5825−5833.
(12) Sisco, S. W.; Moore, J. S. Directional Cyclooligomers via Alkyne Metathesis. *J. Am. Chem. Soc.* **2012**, *134*, 9114−9117.
(13) Zhang, W.; Brombosz, S. M.; Mendoza, J. L.; Moore, J. S. A High-Yield, One-Step Synthesis of o-Phenylene Ethynylene Cyclic Trimer via Precipitation-Driven Alkyne Metathesis. *J. Org. Chem.* **2005**, *70*, 10198−10201.
(14) Zhang, W.; Moore, J. S. Arylene Ethynylene Macrocycles Prepared by Precipitation-Driven Alkyne Metathesis. *J. Am. Chem. Soc.* **2004**, *126*, 12796.
(15) Wang, Q.; Yu, C.; Zhang, C.; Long, H.; Azarnoush, S.; Jin, Y.; Zhang, W. Dynamic covalent synthesis of aryleneethynylene cages through alkyne metathesis: dimer, tetramer, or interlocked complex? *Chem. Sci.* **2016**, *7*, 3370−3376.
(16) Wang, Q.; Yu, C.; Long, H.; Du, Y.; Jin, Y.; Zhang, W. Solution-Phase Dynamic Assembly of Permanently Interlocked Aryleneethynylene Cages through Alkyne Metathesis. *Angew. Chem., Int. Ed.* **2015**, *54*, 7550−7554.
(17) Zhang, C.; Wang, Q.; Long, H.; Zhang, W. A Highly C70 Selective Shape-Persistent Rectangular Prism Constructed through One-Step Alkyne Metathesis. *J. Am. Chem. Soc.* **2011**, *133*, 20995−21001.
(18) Wang, Q.; Zhang, C.; Noll, B. C.; Long, H.; Jin, Y.; Zhang, W. A Tetrameric Cage with D2h Symmetry through Alkyne Metathesis. *Angew. Chem., Int. Ed.* **2014**, *53*, 10663−10667.
(19) Zhou, X.; Thompson, R. R.; Fronczek, F. R.; Lee, S. Size-Selective Synthesis of Large Cycloparaphenyleneacetylene Carbon Nanohoops Using Alkyne Metathesis. *Org. Lett.* **2019**, *21*, 4680−4683.
(20) Bellone, D. E.; Bours, J.; Menke, E. H.; Fischer, F. R. Highly Selective Molybdenum ONO Pincer Complex Initiates the Living Ring-Opening Metathesis Polymerization of Strained Alkynes with Exceptionally Low Polydispersity Indices. *J. Am. Chem. Soc.* **2015**, *137*, 850−856.
(21) Jeong, H.; von Kugelgen, S.; Bellone, D.; Fischer, F. R. Regioselective Termination Reagents for Ring-Opening Alkyne Metathesis Polymerization. *J. Am. Chem. Soc.* **2017**, *139*, 15509−15514.
(22) von Kugelgen, S.; Bellone, D. E.; Cloke, R. R.; Perkins, W. S.; Fischer, F. R. Initiator Control of Conjugated Polymer Topology in Ring-Opening Alkyne Metathesis Polymerization. *J. Am. Chem. Soc.* **2016**, *138*, 6234−6239.
(23) von Kugelgen, S.; Sifri, R.; Bellone, D.; Fischer, F. R. Regioselective Carbyne Transfer to Ring-Opening Alkyne Metathesis

DOI: 10.1021/acs.organomet.9b00430
Organometallics 2019, 38, 4054−4059

Initiators Gives Access to Telechelic Polymers. *J. Am. Chem. Soc.* **2017**, *139*, 7577−7585.
(24) Bunz, U. H. F. Poly(p-phenyleneethynylene)s by Alkyne Metathesis. *Acc. Chem. Res.* **2001**, *34*, 998−1010.
(25) Hu, K.; Yang, H.; Zhang, W.; Qin, Y. Solution processable polydiacetylenes (PDAs) through acyclic enediyne metathesis polymerization. *Chem. Sci.* **2013**, *4*, 3649−3653.
(26) Fürstner, A.; Seidel, G. Ring-Closing Metathesis of Functionalized Acetylene Derivatives: A New Entry into Cycloalkynes. *Angew. Chem., Int. Ed.* **1998**, *37*, 1734−1736.
(27) Fürstner, A.; Guth, O.; Rumbo, A.; Seidel, G. Ring Closing Alkyne Metathesis. Comparative Investigation of Two Different Catalyst Systems and Application to the Stereoselective Synthesis of Olfactory Lactones, Azamacrolides, and the Macrocyclic Perimeter of the Marine Alkaloid Nakadomarin A. *J. Am. Chem. Soc.* **1999**, *121*, 11108−11113.
(28) Hickmann, V.; Alcarazo, M.; Fürstner, A. Protecting-Group-Free and Catalysis-Based Total Synthesis of the Ecklonialactones. *J. Am. Chem. Soc.* **2010**, *132*, 11042−11044.
(29) Beer, S.; Brandhorst, K.; Hrib, C. G.; Wu, X.; Haberlag, B.; Grunenberg, J.; Jones, P. G.; Tamm, M. Experimental and Theoretical Investigations of Catalytic Alkyne Cross-Metathesis with Imidazolin-2-iminato Tungsten Alkylidyne Complexes. *Organometallics* **2009**, *28*, 1534−1545.
(30) Haberlag, B.; Wu, X.; Brandhorst, K.; Grunenberg, J.; Daniliuc, C. G.; Jones, P. G.; Tamm, M. Preparation of Imidazolin-2-iminato Molybdenum and Tungsten Benzylidyne Complexes: A New Pathway to Highly Active Alkyne Metathesis Catalysts. *Chem. - Eur. J.* **2010**, *16*, 8868−8877.
(31) Du, Y.; Yang, H.; Zhu, C.; Ortiz, M.; Okochi, K. D.; Shoemaker, R.; Jin, Y.; Zhang, W. Highly Active Multidentate Ligand-Based Alkyne Metathesis Catalysts. *Chem. - Eur. J.* **2016**, *22*, 7959−7963.
(32) Jyothish, K.; Wang, Q.; Zhang, W. Highly Active Multidentate Alkyne Metathesis Catalysts: Ligand-Activity Relationship and Their Applications in Efficient Synthesis of Porphyrin-Based Aryleneethynylene Polymers. *Adv. Synth. Catal.* **2012**, *354*, 2073−2078.
(33) Jyothish, K.; Zhang, W. Introducing A Podand Motif to Alkyne Metathesis Catalyst Design: A Highly Active Multidentate Molybdenum(VI) Catalyst that Resists Alkyne Polymerization. *Angew. Chem., Int. Ed.* **2011**, *50*, 3435−3438.
(34) Schrock, R. R.; Hoveyda, A. H. Molybdenum and Tungsten Imido Alkylidene Complexes as Efficient Olefin-Metathesis Catalysts. *Angew. Chem., Int. Ed.* **2003**, *42*, 4592−4633.
(35) Ogba, O. M.; Warner, N. C.; O'Leary, D. J.; Grubbs, R. H. Recent advances in ruthenium-based olefin metathesis. *Chem. Soc. Rev.* **2018**, *47*, 4510−4544.
(36) Bindl, M.; Stade, R.; Heilmann, E. K.; Picot, A.; Goddard, R.; Fürstner, A. Molybdenum Nitride Complexes with Ph3SiO Ligands Are Exceedingly Practical and Tolerant Precatalysts for Alkyne Metathesis and Efficient Nitrogen Transfer Agents. *J. Am. Chem. Soc.* **2009**, *131*, 9468−9470.
(37) Heppekausen, J.; Stade, R.; Goddard, R.; Fürstner, A. Practical New Silyloxy-Based Alkyne Metathesis Catalysts with Optimized Activity and Selectivity Profiles. *J. Am. Chem. Soc.* **2010**, *132*, 11045−11057.
(38) Heppekausen, J.; Stade, R.; Kondoh, A.; Seidel, G.; Goddard, R.; Fürstner, A. Optimized Synthesis, Structural Investigations, Ligand Tuning and Synthetic Evaluation of Silyloxy-Based Alkyne Metathesis Catalysts. *Chem. - Eur. J.* **2012**, *18*, 10281−10299.
(39) Lhermet, R.; Fürstner, A. Cross-Metathesis of Terminal Alkynes. *Chem. - Eur. J.* **2014**, *20*, 13188−13193.
(40) Trawny, D.; Quennet, M.; Rades, N.; Lentz, D.; Paulus, B.; Reissig, H. Syntheses, Structures and Conformational Dynamics of 1,3,5-Tris(3″-ethynylbi-phen-yl-2′-yl)benzene Derivatives. *Eur. J. Org. Chem.* **2015**, *2015*, 4667−4674.
(41) Chao, S. T.; Lara, N. C.; Lin, S.; Day, M. W.; Agapie, T. Reversible Halide-Modulated Nickel−Nickel Bond Cleavage: Metal−Metal Bonds as Design Elements for Molecular Devices. *Angew. Chem., Int. Ed.* **2011**, *50*, 7529−7532.
(42) Estes, D. P.; Gordon, C. P.; Fedorov, A.; Liao, W.-C.; Ehrhorn, H.; Bittner, C.; Zier, M. L.; Bockfeld, D.; Chan, K. W.; Eisenstein, O.; Raynaud, C.; Tamm, M.; Coperet, C. Molecular and Silica-Supported Molybdenum Alkyne Metathesis Catalysts: Influence of Electronics and Dynamics on Activity Revealed by Kinetics, Solid-State NMR, and Chemical Shift Analysis. *J. Am. Chem. Soc.* **2017**, *139*, 17597−17607.
(43) Bittner, C.; Ehrhorn, H.; Bockfeld, D.; Brandhorst, K.; Tamm, M. Tuning the Catalytic Alkyne Metathesis Activity of Molybdenum and Tungsten 2,4,6-Trimethylbenzylidyne Complexes with Fluoroalkoxide Ligands OC(CF3)nMe3−n (n = 0−3). *Organometallics* **2017**, *36*, 3398−3406.
(44) O'Reilly, M. E.; Ghiviriga, I.; Abboud, K. A.; Veige, A. S. A New ONO3- Trianionic Pincer-Type Ligand for Generating Highly Nucleophilic Metal−Carbon Multiple Bonds. *J. Am. Chem. Soc.* **2012**, *134*, 11185−11195.
(45) Ehrhorn, H.; Bockfeld, D.; Freytag, M.; Bannenberg, T.; Kefalidis, C. E.; Maron, L.; Tamm, M. Studies on Molybdena- and Tungstenacyclobutadiene Complexes Supported by Fluoroalkoxy Ligands as Intermediates of Alkyne Metathesis. *Organometallics* **2019**, *38*, 1627−1639.
(46) Schrock, R. R.; Pedersen, S. F.; Churchill, M. R.; Ziller, J. W. Formation of cyclopentadienyl complexes from tungstenacyclobutadiene complexes and the x-ray crystal structure of an.eta.3-cyclopropenyl complex, W[C(CMe3)C(Me)C(Me)](Me2NCH2CH2NMe2)Cl3. *Organometallics* **1984**, *3*, 1574−1583.
(47) Churchill, M. R.; Fettinger, J. C.; McCullough, L. G.; Schrock, R. R. Transformation of a tungstenacyclobutadiene complex into a nonfluxional.eta.3-cyclopropenyl complex by addition of a donor ligand. The x-ray structure of the tungstenacyclobutadiene-.eta.3-cyclopropenyl complex W(.eta.5-C5H5)[C3(CMe3)2Me](PMe3)Cl2. *J. Am. Chem. Soc.* **1984**, *106*, 3356−3357.
(48) Schrock, R. R.; Murdzek, J. S.; Freudenberger, J. H.; Churchill, M. R.; Ziller, J. W. Multiple metal-carbon bonds. 39. Preparation of molybdenum and tungsten neopentylidyne complexes of the type M(CCMe3)(O2CR)3, their reactions with acetylenes, and the x-ray structure of the.eta.3-cyclopropenyl complex W[C3(CMe3)Et2](O2CCH3)3. *Organometallics* **1986**, *5*, 25−33.
(49) Hughes, R. P.; Reisch, J. W.; Rheingold, A. L. Oxidative addition of cyclopropenyl cations to zerovalent molybdenum and tungsten centers. Synthesis of.eta.3-cyclopropenyl and.eta.3-oxocyclobutenyl complexes of molybdenum(II) and tungsten(II). Crystal and molecular structures of [Mo(.eta.5-C5H5)(.eta.3-C3Ph2R)(CO)2] (R = Ph, tert-Bu). *Organometallics* **1985**, *4*, 1754−1761.
(50) Drew, M. G. B.; Brisdon, B. J.; Day, A. Cyclopropenyl and oxocyclobutenyl complexes of molybdenum. Crystal and molecular structures of (2,2′-bipyridine)bromodicarbonyl(1—3-η-1,2,3-triphenylcyclopropenyl)molybdenum(II) and (2,2′-bipyridine)-bromodicarbonyl(2—4-η-1-oxo-2,3,4-triphenylcyclobutenyl)-molybdenum(II). *J. Chem. Soc., Dalton Trans.* **1981**, 1310−1316.
(51) Churchill, M. R.; Ziller, J. W.; Pedersen, S. F.; Schrock, R. R. Formation of a tetrahedral WC3 framework from a cyclic WC3-(tungstenacyclobutadiene) system via attack on tungsten by nitrogen-donor ligands: X-ray study of W[C3Me2(But)][Me2N(CH2)-2NMe2]Cl3. *J. Chem. Soc., Chem. Commun.* **1984**, 485−486.
(52) Schrock, R. R. High-oxidation-state molybdenum and tungsten alkylidyne complexes. *Acc. Chem. Res.* **1986**, *19*, 342−348.
(53) Hillenbrand, J.; Leutzsch, M.; Furstner, A. Molybdenum Alkylidyne Complexes with Tripodal Silanolate Ligands: The Next Generation of Alkyne Metathesis Catalysts. *Angew. Chem., Int. Ed.* **2019**, *58*, 15690−15696.

DOI: 10.1021/acs.organomet.9b00430
Organometallics 2019, 38, 4054−4059